

# Modelling the influence of activation-induced apoptosis of CD4<sup>+</sup> and CD8<sup>+</sup> T-cells on the immune system response of a HIV infected patient

Guy-Bart Stan\*, Florence Belmudes#, Raphael Fonteneau#, Frederic Zeggwagh#, Marie-Anne Lefebvre#, Christian Michelet†, Damien Ernst#

**Abstract**—On the basis of the HIV infection dynamics model proposed by ADAMS in [1], we propose an extended model that aims at incorporating the influence of activation-induced apoptosis of CD4<sup>+</sup> and CD8<sup>+</sup> T-cells on the immune system response of HIV infected patients. Through this model we study the influence of this phenomenon on the time evolution of specific cell populations such as plasma concentrations of HIV copies, or blood concentrations of CD4<sup>+</sup> and CD8<sup>+</sup> T-cells. In particular, this study shows that depending on its intensity, the apoptosis phenomenon can either favour or mitigate the long-term evolution of the HIV infection.

**Index Terms**—HIV infection dynamics, activation-induced apoptosis, nonlinear model analysis.

## I. INTRODUCTION

The human Immunodeficiency Virus (HIV) is a retrovirus that may lead to the lethal Acquired Immune Deficiency Syndrome (AIDS). After initial contact and inclusion of the HIV particle into specific types of cell of the immune system, there is a cascade of intracellular events leading to the production of massive numbers of new viral copies, the death of infected cells, and ultimately the devastation of the immune system.

Since the first identification of the disease in 1981, intensive studies have been carried out to understand the fundamental HIV infection mechanisms. HIV primarily infects cells of the human immune system such as helper T-cells (specifically CD4<sup>+</sup> T-cells), macrophages and dendritic cells. When the number of CD4<sup>+</sup> T-cells declines below a critical level, cell-mediated immunity<sup>1</sup> is lost, and the body becomes progressively more susceptible to opportunistic infections. Progression from HIV infection to AIDS is primarily due to an extensive depletion of CD4<sup>+</sup> T-cells.

\*University of Cambridge, Department of Engineering, Control Group, Trumpington Street, Cambridge, CB2 1PZ, United Kingdom; Email: gvs22@eng.cam.ac.uk (Guy-Bart Stan).

#Supélec-IETR, Hybrid Systems Control Group, Rennes, France; Emails: florence.belmudes@gmail.com (Florence Belmudes); raphael.fonteneau@gmail.com (Raphael Fonteneau); frederic.zeggwagh@rennes.supelec.fr (Frederic Zeggwagh); marie-anne.lefebvre@supélec.fr (Marie-Anne Lefebvre); damien.ernst@supélec.fr (Damien Ernst).

†Clinique des Maladies Infectieuses, Unité de Pharmacologie Clinique and Laboratoire de Bactériologie-Virologie, Hôpital Pontchaillou, Rennes, France; Email: christian.michelet@chu-rennes.fr (Christian Michelet).

<sup>1</sup>Cell-mediated immunity is an immune response that does not involve antibodies but rather involves the activation of macrophages, natural killer cells, antigen-specific cytotoxic T-lymphocytes, and the release of various cytokines in response to an antigen.

Several mechanisms are involved in the loss of CD4<sup>+</sup> T-cells and this topic is one of the most controversial issues in recent AIDS research. T-cell loss may be due to direct destruction by the virus (direct virus-induced cytolysis) or to defective T-cell generation. In 1991, apoptosis, also called programmed cell death, has been suggested as another mechanism responsible for T-cell depletion during the evolution of HIV-1 infection and an extensive body of recent literature is supporting this hypothesis ([2], [3], [4], [5], [6]). In HIV-infected patients, both infected and uninfected cells undergo accelerated apoptosis but, remarkably, the vast majority of the cells that undergo apoptosis are uninfected ([7]). Furthermore, the level of apoptosis in HIV-1 infected patients is correlated to the levels of circulating CD4<sup>+</sup> T-cells and the stage of disease ([7]), which reinforces the idea that apoptosis induced by the HIV infection plays an important role in the death of the lymphocytes.

Mathematical analysis of the HIV/AIDS infection is actively studied since the middle of the 90's. Several authors have proposed mathematical models to describe the HIV infection dynamics (e.g. [1], [8], [9], [10], [11], [12]). These models are often represented by a set of nonlinear Ordinary Differential Equations (ODEs) which model the long-term interaction between the immune system and the virus. They generally take into consideration several biological phenomena that influence the infection process, but, to the best of our knowledge, no mathematical model has yet tried to explain the influence of the activation-induced apoptosis phenomenon on the HIV infection dynamics.

In this paper, we propose a modification of the model proposed by ADAMS et al. in [1]. This modification aims at modelling the activation-induced apoptosis phenomenon and analyse its influence on the HIV infection dynamics. Similarly to the model initially proposed by Adams et al., our model is characterised by different equilibrium points and does not directly aim at predicting the long-term collapse of the immune system, which may be due to several factors such as virus mutations or fatigue of the immune system resulting in progressive thymus degradation.

The paper is organised as follows. Section II introduces our proposed mathematical model for the influence of apoptosis on the HIV infection dynamics. In Section III we analyse the properties of this model by relying both on simulations and nonlinear bifurcation analysis. Finally, we discuss the implications and limitations of the proposed model in Section IV.

## II. APOPTOSIS-COMPLIANT MODEL FOR THE HIV INFECTION DYNAMICS

Section II-A briefly describes the model of ADAMS et al. introduced in [1]. Based on this model, we propose in Section II-B an extension which takes into account the activation-induced apoptosis phenomenon.

### A. The model of ADAMS et al.

The model of ADAMS et al. introduced in [1] is a compartmental ordinary differential equation model in which each compartment corresponds to a specific type of cell population. The model predicts the time evolution of specific cell populations such as for example blood concentrations of CD4<sup>+</sup> T-lymphocytes and plasma concentration of HIV virions. More specifically, it is described by the following set of ordinary differential equations<sup>2</sup>

$$\dot{T}_1 = \lambda_1 - d_1 T_1 - k_1 V T_1 \quad (1)$$

$$\dot{T}_2 = \lambda_2 - d_2 T_2 - k_2 V T_2 \quad (2)$$

$$\dot{T}_1^* = k_1 V T_1 - \delta T_1^* - m_1 E T_1^* \quad (3)$$

$$\dot{T}_2^* = k_2 V T_2 - \delta T_2^* - m_2 E T_2^* \quad (4)$$

$$\dot{V} = N_T \delta (T_1^* + T_2^*) - c V \quad (5)$$

$$\begin{aligned} \dot{E} = & \lambda_E + \frac{b_E (T_1^* + T_2^*)}{(T_1^* + T_2^*) + K_b} E \\ & - \frac{d_E (T_1^* + T_2^*)}{(T_1^* + T_2^*) + K_d} E - \delta_E E \end{aligned} \quad (6)$$

where  $T_1$  ( $T_1^*$ ) denotes the number of non-infected (infected) CD4<sup>+</sup> T-lymphocytes (in *cells/ml*),  $T_2$  ( $T_2^*$ ) the number of non-infected (infected) macrophages (in *cells/ml*),  $V$  the number of free HIVs (in *virions/ml*) and  $E$  the number of HIV-specific cytotoxic CD8<sup>+</sup> T-cells (in *cells/ml*).

The values of the different parameters of the model are taken from [1]:  $\lambda_1 = 10,000$  ( $\frac{\text{cells}}{\text{ml} \times \text{day}}$ ),  $d_1 = 0.01$  ( $\frac{1}{\text{day}}$ ),  $k_1 = 8 \times 10^{-7}$  ( $\frac{\text{ml}}{\text{virions} \times \text{day}}$ ),  $\lambda_2 = 31.98$  ( $\frac{\text{cells}}{\text{ml} \times \text{day}}$ ),  $d_2 = 0.01$  ( $\frac{1}{\text{day}}$ ),  $f = 0.34$ ,  $k_2 = 10^{-4}$  ( $\frac{\text{ml}}{\text{virions} \times \text{day}}$ ),  $\delta = 0.7$  ( $\frac{1}{\text{day}}$ ),  $m_1 = 10^{-5}$  ( $\frac{\text{ml}}{\text{cells} \times \text{day}}$ ),  $m_2 = 10^{-5}$  ( $\frac{\text{ml}}{\text{cells} \times \text{day}}$ ),  $N_T = 100$  ( $\frac{\text{virions}}{\text{cells}}$ ),  $c = 13$  ( $\frac{1}{\text{day}}$ ),  $\rho_1 = 1$  ( $\frac{\text{virions}}{\text{cells}}$ ),  $\rho_2 = 1$  ( $\frac{\text{virions}}{\text{cells}}$ ),  $\lambda_E = 1$  ( $\frac{\text{cells}}{\text{ml} \times \text{day}}$ ),  $b_E = 0.3$  ( $\frac{1}{\text{day}}$ ),  $K_b = 100$  ( $\frac{\text{cells}}{\text{ml}}$ ),  $d_E = 0.25$  ( $\frac{1}{\text{day}}$ ),  $K_d = 500$  ( $\frac{\text{cells}}{\text{ml}}$ ),  $\delta_E = 0.1$  ( $\frac{1}{\text{day}}$ ).

As a general remark, some side simulations have shown that all the results presented in this paper are qualitatively robust with respect to perturbations of the nominal parameter values listed above. We therefore, only consider these nominal values in the presented results.

In order to provide insight into the properties of this model, we briefly discuss its main characteristics.

<sup>2</sup>The model proposed in [1] also includes two control inputs representing the effect of the two main types of drugs (Protease Inhibitors and Reverse Transcriptase Inhibitors) typically used in Highly Active Anti-Retroviral Therapy (HAART). In this paper, we specifically focus on the mathematical modelisation of activation-induced apoptosis for non-treated patients and therefore do not consider these two control inputs.

As shown in [1], the system of ordinary differential equations (1)-(6) exhibits four physical equilibrium points (and several non physical ones, omitted here, for which one or several state variables are negative). The first three physical equilibrium points have a clear biological interpretation. The fourth equilibrium point has no clear biological interpretation and can be shown to be locally unstable. Nevertheless this latter equilibrium point plays an important role in the apoptosis-compliant dynamics as we will discuss later in Section III.

These physical equilibrium points are respectively

- 1) an uninfected unstable equilibrium point

$$\begin{aligned} & (T_1, T_2, T_1^*, T_2^*, V, E)_{eq} \\ & = (10^6, 3198, 0, 0, 0, 10) \end{aligned}$$

- 2) an infected, so-called ‘‘healthy’’, locally stable equilibrium point

$$\begin{aligned} & (T_1, T_2, T_1^*, T_2^*, V, E)_{eq} \\ & = (967839, 621, 76, 6, 415, 353104) \end{aligned}$$

which corresponds to a small viral load, a high CD4<sup>+</sup> T-lymphocytes count and a high HIV-specific cytotoxic T-cells count,

- 3) an infected, so-called ‘‘non-healthy’’, locally stable equilibrium point

$$\begin{aligned} & (T_1, T_2, T_1^*, T_2^*, V, E)_{eq} \\ & = (163573, 5, 11945, 46, 63919, 24) \end{aligned}$$

for which T-cells are depleted and the viral load is very high.

- 4) an infected locally unstable equilibrium point

$$\begin{aligned} & (T_1, T_2, T_1^*, T_2^*, V, E)_{eq} \\ & = (664938, 50, 1207, 11, 6299, 207658) \end{aligned}$$

Numerical simulations show that the basin of attraction of the ‘‘healthy’’ steady-state is relatively small in comparison with the one of the ‘‘non-healthy’’ steady-state. Furthermore, perturbation of the uninfected steady-state by adding as less as one single HIV per *ml* of blood plasma leads to asymptotic convergence towards the ‘‘non-healthy’’ steady-state as can be seen in Figure 1.

### B. Incorporation of the apoptosis phenomenon into the model of ADAMS et al.

Apoptosis, also called programmed cell death, is a process of deliberate life relinquishment by a cell in a multicellular organism. It is an important biological process whose main goal is to eliminate selected cells for the benefit of the whole organism. Apoptosis can, for example, occur when a cell is damaged beyond repair, infected with a virus, or undergoing stress conditions such as starvation. The ‘‘decision’’ for apoptosis can either come from the cell itself, or be induced from its surrounding environment (see [13] for a general introduction on apoptosis).

In the special case of lymphocytes, apoptosis plays an important role in optimising the functions of the immune system by compensating lymphocytes proliferation through the elimination of cells that have become ill or ineffective.

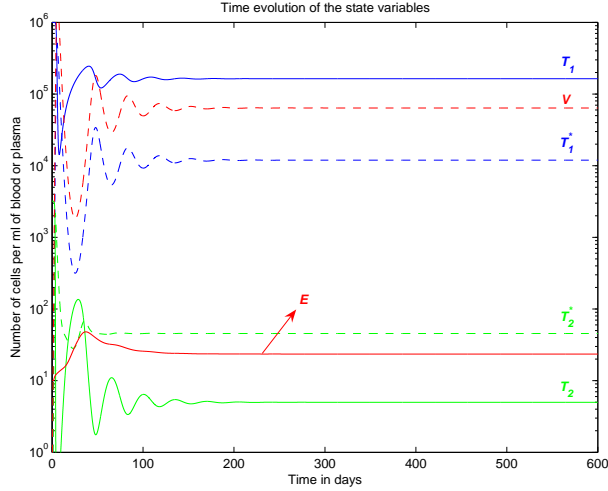


Fig. 1. Time evolution of the state variables of the model (1)-(6) starting from the primo-infection initial condition  $(T_1, T_2, T_1^*, T_2^*, V, E) = (10^6, 3198, 0, 0, 1, 10)$ .

When apoptosis is not influenced by the presence of other cells, its effect can be considered as constant during the HIV infection, i.e. the death rates of the cells related to apoptosis does not change with the evolution of the disease. In such a context, apoptosis is generally included in the natural death rate of each cell (represented by the terms  $-d_1T_1$ ,  $-d_2T_2$ ,  $-\delta_E E$  and, to a certain extent,  $-\delta T_1^*$  and  $-\delta T_2^*$  in the model (1)-(6)). However, this is cannot be the case for environment dependent apoptosis. Indeed, as reported in [2] and [5], lymph nodes of HIV-infected individuals contain a high percentage (with respect to uninfected individuals) of uninfected CD4<sup>+</sup> and CD8<sup>+</sup> cells which are in an apoptotic state – that is which are ready to enter into an apoptotic process. Furthermore, these studies also showed that the apoptosis rates of these apoptotic cells were dependent on the stage of evolution of the HIV infection, and more specifically on the number of infected cells. As a general conclusion of these observations, the per-day proportion of uninfected but apoptotic CD4<sup>+</sup> and CD8<sup>+</sup> T-cells must be dependent on the number of infected cells and thus cannot be represented by constant factors ( $d_1$ ,  $d_2$ ,  $\delta_E$ , or  $\delta$ ) as is the case for spontaneous apoptosis.

From a biological point of view, uninfected CD4<sup>+</sup> and CD8<sup>+</sup> T-cells have been shown to be prematurely marked for apoptosis due to the presence of biochemical messengers, for example the glycoprotein gp120, one of the most well established apoptosis-inducing factor ([3], [4]). As summarised in [14] and [15], there are several main potential sources for apoptosis-inducing factors: infected cells or free virus particles expressing gp120 on their surface, soluble gp120 alone, and Tat viral proteins. Other viral proteins, such as the accessory protein Nef [16] and possibly the immediate-early protein Vpr [17] may also induce apoptosis. Furthermore, some references (e.g. [3]) suggest the existence of a two step mechanism in which, firstly, T-cells are primed for a premature death by interaction with gp120, and secondly, the actual death signal is delivered by membrane-bound TNF-alpha on the surface of

macrophages.

For the sake of obtaining a model which is able to qualitatively capture the activation-induced apoptosis phenomenon without becoming too complex for its analysis, we assume that all the potential apoptosis-inducing factors are directly correlated with the concentration of HIV-infected CD4<sup>+</sup> T-cells ( $T_1^*$ ) and that the activation-induced apoptosis signalling does not involve macrophages. Finally, we assume that the per-day apoptosis proportions depend linearly on the concentration of infected CD4<sup>+</sup> T-cells<sup>3</sup>.

Consequently, we propose the following modification of the non-infected CD4<sup>+</sup> T-cells dynamics:  $\dot{T}_1 = \lambda_1 - d_1T_1 - k_1VT_1 - \delta_{T_1}T_1$  where  $\delta_{T_1}$  (expressed in  $\frac{1}{day}$ ) denotes the activation-induced apoptosis proportion of non-infected CD4<sup>+</sup> T-cells. According to our previously described assumptions, we assume that  $\delta_{T_1}$  depends solely on  $T_1^*$ , i.e.  $\dot{T}_1 = \lambda_1 - d_1T_1 - k_1VT_1 - \delta_{T_1}(T_1^*)T_1$ . Finally, assuming this dependence on  $T_1^*$  to be linear, we obtain that  $\delta_{T_1}(T_1^*) = a_{T_1}T_1^*$  where  $a_{T_1}$  is a non negative parameter (expressed in  $\frac{ml}{cells \times day}$ ) called the activation-induced apoptosis parameter of uninfected CD4<sup>+</sup> T-cells when in presence of infected CD4<sup>+</sup> T-cells (or apoptosis parameter for short). A similar modification is considered for the dynamics of CD8<sup>+</sup> cells. The corresponding modified model writes:

$$\dot{T}_1 = \lambda_1 - d_1T_1 - k_1VT_1 - a_{T_1}T_1^*T_1 \quad (7)$$

$$\dot{T}_2 = \lambda_2 - d_2T_2 - k_2VT_2 \quad (8)$$

$$\dot{T}_1^* = k_1VT_1 - \delta T_1^* - m_1ET_1^* \quad (9)$$

$$\dot{T}_2^* = k_2VT_2 - \delta T_2^* - m_2ET_2^* \quad (10)$$

$$\dot{V} = N_T\delta(T_1^* + T_2^*) - cV \quad (11)$$

$$\begin{aligned} \dot{E} = & \lambda_E + \frac{b_E(T_1^* + T_2^*)}{(T_1^* + T_2^*) + K_b}E \\ & - \frac{d_E(T_1^* + T_2^*)}{(T_1^* + T_2^*) + K_d}E - \delta_E E - a_E T_1^* E \end{aligned} \quad (12)$$

where  $a_{T_1}$  and  $a_E$  are expressed in  $\frac{ml}{cells \times day}$ .

### III. ANALYSIS OF THE APOPTOSIS-COMPLIANT MODEL

In this section, we analyse the HIV infection dynamics model described by the system of ODEs (7)-(12). This analysis mainly focuses on the study of the influence of the apoptosis parameters  $a_{T_1}$  and  $a_E$  on the modelled dynamics.

In order to study the influence of some parameters on the dynamics of a nonlinear system modelled by ODEs, one generally relies on a combination of two complementary

<sup>3</sup>It would also, for example, make sense to consider that the infected CD4<sup>+</sup> T-cells, macrophages, and free HIV are correlated with the apoptosis-inducing factors. However, some side simulations and analysis not reported in this paper, have shown that replacing the term  $a_{T_1}T_1^*$  by the term  $a_{T_1}(\alpha T_1^* + \beta T_2^* + (1 - \alpha - \beta)V)$  with  $\alpha, \beta \in [0, 1]$  and  $\alpha + \beta = 1$  yields results which are qualitatively quite similar. This can be explained by the fact that the time evolutions of infected CD4<sup>+</sup> T-cells, macrophages, and virions predicted by our model are highly correlated. The main reason for having adopted the simpler term  $a_{T_1}T_1^*$  was to obtain a model which could capture the fundamental dynamics associated with the activation-induced apoptosis phenomenon, while, at the same time, being simple enough to lend itself to a detailed analysis.

approaches. The first one is a simulation based approach which consists in numerically integrating the set of ODEs for different values of the system parameters (and often also for different initial conditions). The second one is more analytical and relies on a bifurcation analysis of the system with respect to the parameters of interest. This second approach aims at establishing the influence of the parameters of interest on the number, the stability and the position of the attractors of the system.

More specifically, the simulation part allows us to identify typical asymptotic behaviours exhibited by the proposed model and to determine the time needed to reach a specific neighbourhood of these asymptotic behaviours. On the other hand the bifurcation analysis provides a better insight into the dynamic mechanisms that correlate the apoptosis parameters  $a_{T_1}$  and  $a_E$  with these asymptotic behaviours.

For the sake of simplicity, the analysis will start by considering that  $a_E$  is equal to zero which is equivalent to neglecting activation-induced apoptosis in the dynamics of CD8<sup>+</sup> T-cells. Afterwards, we study the case where both  $a_{T_1}$  and  $a_E$  are different from zero. To lighten the presentation of the results, we will mainly consider in our study a single initial state corresponding to the primo-infection point  $(T_1, T_2, T_1^*, T_2^*, V, E) = (10^6, 3198, 0, 0, 1, 10)$  and limit the range of values for  $a_{T_1}$  and  $a_E$  to  $[0, 1]$ . While this may seem to be restrictive, we found that the qualitative nature of our results were very robust with respect to “biologically plausible” initial conditions. Furthermore, we believe that for values of  $a_{T_1}$  and  $a_E$  greater than 1, the modelled activation-induced apoptosis rates become so important that they cannot remain in adequacy with reality. Indeed, such high values of the apoptosis parameters would yield an almost complete depletion of the T-cells within less than a few minutes.

#### A. Simulation results for $a_{T_1} \in [0, 1]$ and $a_E = 0$

By numerically integrating the model (7)-(12) starting from various initial conditions for different values of  $a_{T_1} \in [0, 1]$ , we have always observed convergence to an equilibrium point. However, the position of this equilibrium was found to be highly dependent on the value of the apoptosis parameter  $a_{T_1}$ . For  $0 \leq a_{T_1} \leq 3.874 \times 10^{-5}$ , this position evolves continuously when the values of  $a_{T_1}$  are increased, and remains very close to the position of the “non-healthy” equilibrium point corresponding to  $a_{T_1} = 0$ . At the particular threshold value  $a_{T_1} = 3.874 \times 10^{-5}$ , there is a sudden “jump” towards a new position for which the corresponding asymptotic values of the state variables can be associated to a “healthier” situation, i.e. the viral load and infected cells concentrations are drastically decreased while the non-infected and HIV-specific cytotoxic T-cells concentrations are significantly increased. However, beyond the threshold value  $a_{T_1} = 3.874 \times 10^{-5}$ , this previously described healthier situation steadily degrades with increasing values of  $a_{T_1}$ . For values of  $a_{T_1}$  greater than say  $10^{-3}$ , convergence to a point which is “less healthy” than the “non-healthy” equilibrium point described in Section II-A occurs.

In Figure 2, we represent three typical time evolutions for the state variables of the model (7)-(12) when starting from the

primo-infection point. These three time evolutions correspond to the following apoptosis parameter values  $a_{T_1} = 10^{-5}$ ,  $a_{T_1} = 10^{-4}$ , and  $a_{T_1} = 10^{-2}$ , respectively.

Up to this point, we have mainly focused on the study of the properties of the system (7)-(12) in asymptotic conditions. However, as illustrated in Figure 3, the time needed to reach a close neighbourhood of the asymptotic equilibrium values may be large<sup>4</sup>. In particular, the time needed for the state-space trajectories to reach a neighbourhood of the equilibrium point to which they asymptotically converge is significantly increasing around the threshold value  $a_{T_1} = 3.874 \times 10^{-5}$ . This latter observation together with the fact that during the transient period the state variables deviation with respect to their asymptotic value may be significant (see Figure 2) show that the transient dynamics and settling-time must also be taken into consideration when studying the effects of activation-induced apoptosis.

In order to get a better insight into the influence of the apoptosis parameter  $a_{T_1}$  on the dynamics of the proposed model, and especially to understand why there exists a range of values for  $a_{T_1}$  for which the patient state converges to an equilibrium point which is significantly “healthier” than the “non-healthy” equilibrium point described in Section II, we perform, in Section III-B, a detailed bifurcation analysis.

#### B. Bifurcation analysis for $a_{T_1} \in [0, 1]$ and $a_E = 0$

We performed a bifurcation analysis of the equilibrium points of the model (7)-(12) by relying on the numerical tool MATCONT<sup>5</sup> [18]. The results of this bifurcation analysis are given in Figure 4 where the physical infected equilibrium point values of  $T_1$  are represented as a function of the apoptosis parameter  $a_{T_1}$ . The unstable uninfected equilibrium point value of  $T_1$  is independent of  $a_{T_1}$  and is thus not represented.

This bifurcation diagram helps in understanding the different observed behaviours. For values of  $a_{T_1}$  in the range  $[0, 3.874 \times 10^{-5}[$ , three equilibrium points coexist, two of them are locally stable (eq. point 1 and eq. point 2) while the remaining one is unstable. The asymptotic behaviour of the system depends on the chosen initial condition for the model. Performing simulations for a large number of “biologically plausible” initial conditions, we have always observed convergence to one of the two locally stable equilibrium points. Furthermore, considering  $a_{T_1} \in [0, 3.874 \times 10^{-5}[$  and starting from the primo-infection initial condition or a perturbed version of this initial condition<sup>6</sup>, convergence to the “non-healthy” stable equilibrium point (eq. point 2) has always

<sup>4</sup>Some side simulations have shown that a significant increase in the settling-time values around the bifurcation threshold always occurs independently of the chosen initial condition. Therefore, the results presented in Figure 3 for the primo-infection initial condition can be considered as representative for any initial condition.

<sup>5</sup>MATCONT is a MATLAB toolbox incorporating various numerical differential equation solvers and continuation algorithms for bifurcation analysis. It is freely available at <http://www.matcont.ugent.be/>.

<sup>6</sup>During the simulations, we have considered perturbations for which the initial concentrations are defined as  $(k_1 T_{1pi}, k_2 T_{2pi}, k_3 T_{1pi}^*, k_4 T_{2pi}^*, k_5 V_{pi}, k_6 E_{pi})$  with  $k_i, i = 1, \dots, 6$  randomly chosen in the interval  $[0.75, 1.25]$  and  $(T_{1pi}, T_{2pi}, T_{1pi}^*, T_{2pi}^*, V_{pi}, E_{pi}) = (10^6, 3198, 0, 0, 1, 10)$ .

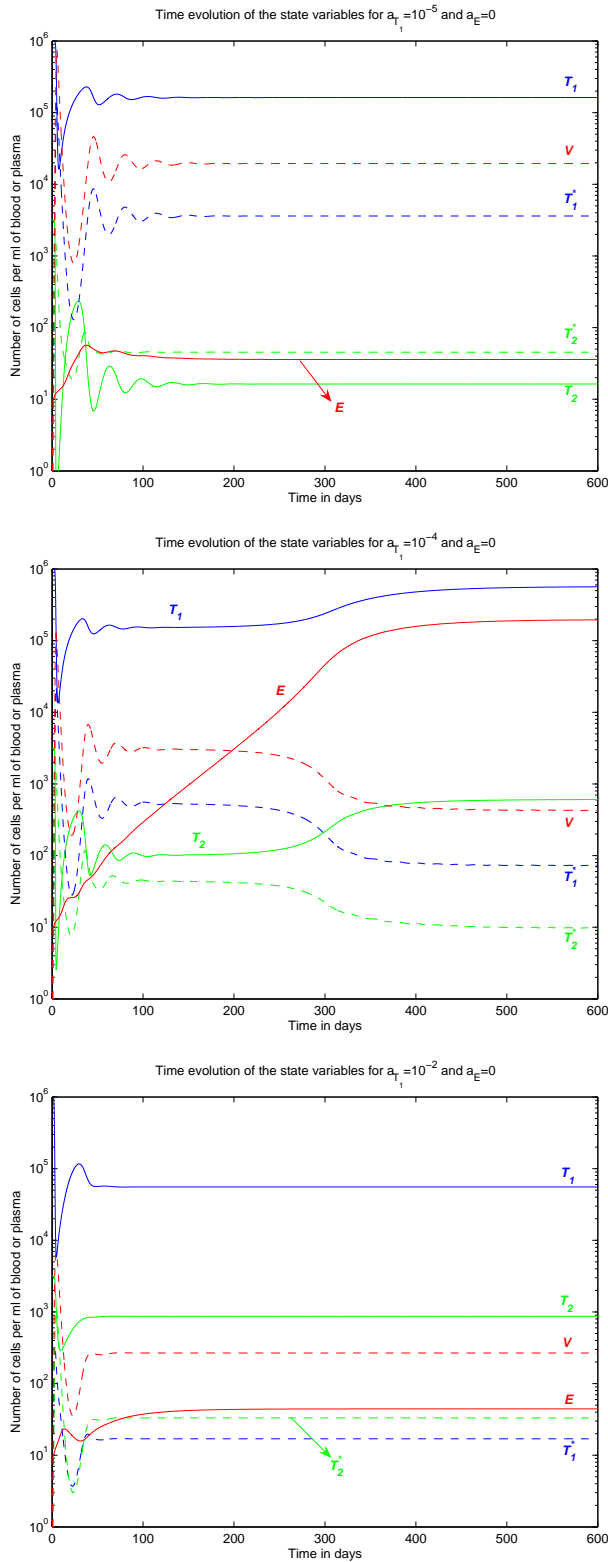


Fig. 2. Time-evolution of the state variables of the model (7)-(12) for different values of the apoptosis parameter  $a_{T_1}$ :  $a_{T_1} = 10^{-5}$  (top),  $a_{T_1} = 10^{-4}$  (middle), and  $a_{T_1} = 10^{-2}$  (bottom). For every graph, the model has been numerically integrated starting from the primo-infection initial condition  $(T_1, T_2, T_1^*, T_2^*, V, E) = (10^6, 3198, 0, 0, 1, 10)$  and the effect of activation-induced apoptosis on the dynamics of the CD8<sup>+</sup> T-cells has been neglected (i.e.,  $a_E = 0$ ).

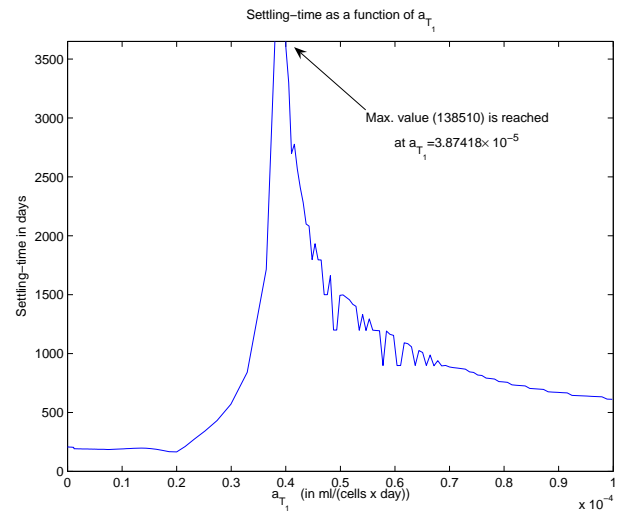


Fig. 3. Evolution of the settling-time as a function of the apoptosis parameter  $a_{T_1}$ , when starting from the primo-infection initial condition and considering  $a_E = 0$ . The settling-time is defined as the minimum time required for the state variables to be within an infinite-norm distance of 1 percent of their asymptotic value. The maximum settling-time value (138510 days) is reached at the threshold value  $a_{T_1} = 3.87418 \times 10^{-5}$ .

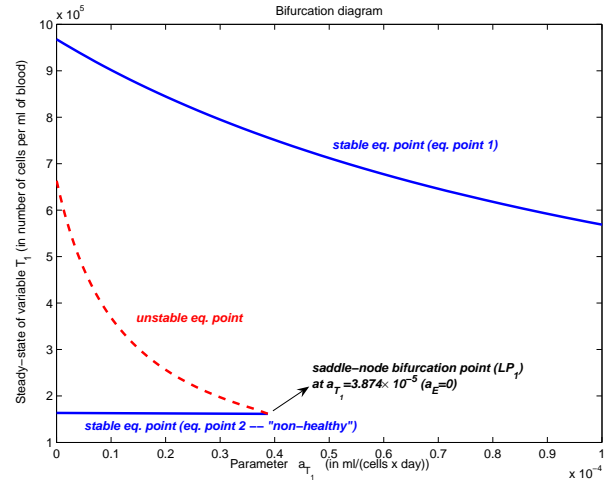


Fig. 4. Bifurcation diagram of the equilibrium concentrations of non-infected CD4<sup>+</sup> T-cells ( $T_{1eq}$ ) when the bifurcation parameter  $a_{T_1}$  varies from 0 to  $10^{-4}$ . A saddle-node bifurcation point ( $LP_1$ ) exists at  $a_{T_1} = 3.874 \times 10^{-5}$ . Only the infected equilibrium points (equilibrium points 2, 3 and 4) are represented and  $a_E$  is chosen equal to 0. The equilibrium points at  $a_{T_1} = 0$  correspond to the three infected equilibrium points of the model (1)-(6) described in Section II-A.

been observed. This latter observation confirms that the basin of attraction of the “healthy” equilibrium point (eq. point 1) is much smaller when compared to the one of the “non-healthy” equilibrium point (eq. point 2). At  $a_{T_1} = 3.874 \times 10^{-5}$ , the “non-healthy” equilibrium point (eq. point 2) coalesces with the unstable one through a saddle-node (also called limit point) bifurcation. We denote this point by  $LP_1$  where  $LP$  stands for limit point. For values of  $a_{T_1}$  in the range  $[3.874 \times 10^{-5}, 1]$ , a single locally stable equilibrium point exists (eq. point 1). Furthermore, as  $a_{T_1}$  increases towards 1, the position of this locally stable equilibrium (eq. point 1) evolves in such a

way that  $T_{1_{eq}}$ ,  $T_{2_{eq}}$  and  $E_{eq}$  decrease while  $T_{1_{eq}}^*$ ,  $T_{2_{eq}}^*$  and  $V_{eq}$  increase, explaining the previously simulation-observed degradation in the patient state.

*Remark:* If one performs a bifurcation analysis for negative values of  $a_{T_1}$ , a second saddle-node bifurcation point appears, where eq. point 1 coalesces with the unstable equilibrium point. We denote this point by  $LP_2$ . This point  $LP_2$  has not been represented in Figure 4 since negative values of  $a_{T_1}$  make no biological sense in our model. Nevertheless noticing the existence of this second saddle-node bifurcation point is important in order to understand the two-parameter bifurcation analysis presented in Section III-C.

C. Analysis for  $a_{T_1} \in [0, 1]$  and  $a_E \in [0, 1]$

In this section, we additionally include the effect of activation-induced apoptosis on the  $CD8^+$  T-lymphocytes and thus consider the model (7)-(12) where both  $a_{T_1}$  and  $a_E$  may take non-zero values. We first describe the results of a bifurcation analysis encompassing both the parameters  $a_{T_1}$  and  $a_E$ . Afterwards, we discuss the additional information that simulations can bring with respect to this analysis. This two-parameter bifurcation analysis is based on a numerical continuation of the saddle-node bifurcation point  $LP_1$  occurring at  $(a_{T_1}, a_E) = (3.874 \times 10^{-5}, 0)$  (see [19], [20] for details about the continuation algorithm used). The corresponding two-parameter continuation diagram is given in Figure 5. On this latter figure, we can see that a CUSP bifurcation point<sup>7</sup> exists at  $(a_{T_1}, a_E) = (4.838 \times 10^{-4}, 1.956 \times 10^{-4})$ . At this point two branches,  $LP_1$  and  $LP_2$ , of saddle-node bifurcation curves meet tangentially. These two branches divide the parameter plane into two regions. Inside the wedge between  $LP_1$  and  $LP_2$ , there are three equilibria, two stable (eq. points 1 and 2) and one unstable. Outside the wedge, there is a single equilibrium, which is stable. This equilibrium point may be either eq. point 1 or eq. point 2 depending if we are below  $LP_1$  or above  $LP_2$ . If we approach the CUSP point from inside the  $LP_1$ - $LP_2$  wedge, all three equilibria merge together so that only a single stable equilibrium point remains beyond the CUSP bifurcation point.

To obtain a clear understanding of the influence of the two activation-induced apoptosis parameters  $a_{T_1}$  and  $a_E$  on the set of reached equilibrium points when starting from the primo-infection initial condition we consider the 3D plot given in Figure 6.

Figure 6 represents for different values of  $(a_{T_1}, a_E)$  the value of  $T_1$  corresponding to the equilibrium point to which the patient's state converges when starting from the primo-infection initial condition. Similarly to what we observed in Section III-B, we see that there exist ranges of values of  $a_{T_1}$  and  $a_E$  where activation-induced apoptosis can have a beneficial effect that hinders the progression of the HIV infection. These values are located below the  $LP_1$  curve in the  $(a_{T_1}, a_E)$ -plane (see Figure 5). For any fixed value of  $a_E$  in

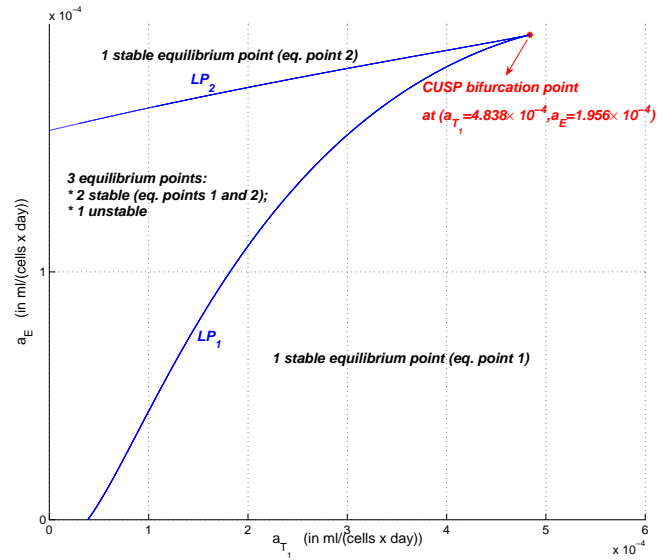


Fig. 5. Two-parameter continuation of the saddle-node bifurcation point  $LP_1$  corresponding to  $(a_{T_1}, a_E) = (3.87418 \times 10^{-5}, 0)$ . A CUSP bifurcation point appears at  $(a_{T_1}, a_E) = (4.838 \times 10^{-4}, 1.956 \times 10^{-4})$ .

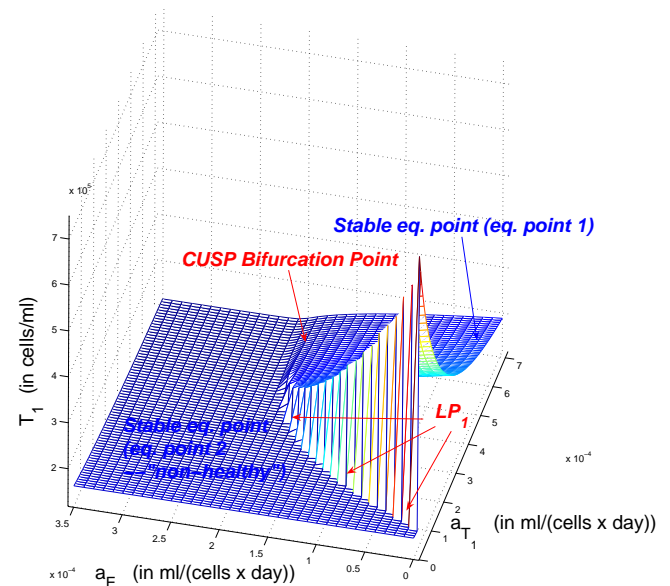


Fig. 6. Concentrations of non-infected  $CD4^+$  T-cells ( $T_1$ ) corresponding to the equilibrium point to which the patient's state converges when starting from the primo-infection initial condition. The saddle-node bifurcation curve  $LP_2$  is not visible since starting from the primo-infection initial condition all trajectories corresponding to  $(a_{T_1}, a_E)$ -values inside the  $LP_1$ - $LP_2$  wedge converge to the “non-healthy” stable equilibrium point (eq. point 2).

<sup>7</sup>At the CUSP bifurcation point two branches of saddle-node bifurcation curves meet tangentially. For nearby parameter values, the system can have three equilibria which collide and disappear pairwise via the saddle-node bifurcations.

the range  $[0, 1.956 \times 10^{-4}]$ , by increasing the value of  $a_{T_1}$  just above the corresponding threshold value defined by the  $LP_1$  curve, there is a sudden change in the value of  $T_1$  associated with the convergence point. This is due to the fact that below the  $LP_1$  curve given in Figure 5, the system converges to an equilibrium point parented with the “healthy” equilibrium point (eq. point 1), as defined in Section III-A, while above this curve it converges to a point parented with the “non-healthy” equilibrium (eq. point 2). Increasing the value of  $a_{T_1}$  further beyond this  $LP_1$ -defined threshold value, the “healthiness” (measured in proportion with the corresponding value of  $T_{1eq}$ ) of the convergence point decreases with increasing values of  $a_{T_1}$ . It is also important to notice that for any value of  $a_{T_1}$ , the “healthiness” of the convergence point always decreases with  $a_E$ . These two parameters do not have the same effect on the HIV infection as can be seen from the asymmetry of the graphs given in Figures 5 and 6. Actually, this can be explained by the fact that the death of  $CD4^+$  T-cells by activation-induced apoptosis can mitigate the HIV infection by limiting the number of cells in which the HIV can copy itself while this is not the case for  $CD8^+$  T-cells since they are not directly targeted by HIVs in our model. Also, and similar to what we showed in Section III-A, we found that the settling time, i.e. the time needed to reach a small neighbourhood of the asymptotically reached equilibrium point, becomes particularly large for  $(a_{T_1}, a_E)$  values located close to the  $LP_1$  curve.

#### IV. DISCUSSION

Based on the HIV infection dynamics model proposed by ADAMS in [1], we have proposed an extended model which aims at incorporating the apoptosis-inducing effects that the HIV infection has on non-infected  $CD4^+$  and  $CD8^+$  T-cells.

The part of this model specific to these activation-induced apoptosis phenomena depends upon two apoptosis parameters which determine its magnitude ( $a_{T_1}$  and  $a_E$ ). Using a combination of numerical simulations and bifurcation analysis, we found that for some ranges of values of these parameters, these activation-induced apoptosis phenomena could have some beneficial effects on the control of the HIV infection. Indeed, in those ranges, the effect of activation-induced apoptosis modifies the time evolution of the  $CD4^+$  T-cells concentrations in a way which is particularly beneficial for preserving the immune system integrity. On the other hand, when the magnitude of the apoptosis parameters becomes too large, this potential beneficial effect disappears and activation-induced apoptosis mechanisms were then found to aggravate the HIV infection. Furthermore, since the HIV infection worsens when these activation-induced apoptosis rates become too large, one could also relate the progression of the HIV infection to AIDS to a change of magnitude in these rates. These findings need to be taken with caution since they are dependent on several modelling assumptions (per-day apoptosis proportions are linearly proportional to the concentration of infected  $CD4^+$  cells and the propensity non-infected  $CD4^+$  and  $CD8^+$  cells have to undergo apoptosis is proportional to their concentration) that would certainly require careful experimental validation.

We emphasise that these results could also potentially help in designing new anti-HIV therapies based on a drug-mediated regulation of the activation-induced apoptosis factors (such as gp120) in HIV infected patients. These therapies could be based on the injection of some specific interleukins<sup>8</sup> to HIV positive patients, such as for example IL-2, IL-7 and IL-15. Indeed, the anti-apoptotic effect of these interleukins has been reported in the literature [14], [21], [7]. For example, reference [14] suggests that IL-15 could be used as an immunorestorative agent in HIV treatment because of its anti-apoptotic properties, and its role in enhancing survival and functions of  $CD8^+$  T-cells. Also, the in-vitro results presented in [7] highlight the beneficial anti-apoptotic effects of IL-2 and IL-7 on  $CD4^+$  and  $CD8^+$  T-cells of HIV infected patients. However, the role of interleukins on the immune system of HIV-infected patients/monkeys is still a controversial issue since other studies (see e.g. [22]) have shown that they could have a detrimental effect. Nevertheless, these contradictory results concerning the effects of interleukins on the HIV infection could potentially be explained by the analysis of our extended model, which shows that a decrease in apoptosis rates does not necessarily lead to a better immune system response.<sup>9</sup>

Finally, we acknowledge that the model proposed in this paper possesses some limitations. In particular, similarly to the model initially proposed by ADAMS et al., our model is not able to predict the in-vivo observed long-term collapse of the immune system, which may be due to several factors such as virus mutations, or fatigue of the immune system resulting in progressive thymus degradation. In ongoing research we investigate some modifications of the proposed model to overcome these limitations. Also, our model does not encompass the effects of Highly Active Anti-Retroviral (HAART) drugs and of activation-induced apoptosis on the HIV dynamics. More research would certainly be useful to explore ways to design models that overcome these two limitations.

#### REFERENCES

- [1] B. Adams, H. Banks, H.-D. Kwon, and H. Tran, “Dynamic multidrug therapies for HIV: Optimal and STI control approaches,” *Mathematical Biosciences and Engineering*, vol. 1, no. 2, pp. 223–241, September 2004.
- [2] G. Pantaleo and A. S. Fauci, “Apoptosis in HIV infection,” *Nature Medicine*, vol. 1, no. 2, pp. 118–120, February 1995. [Online]. Available: <http://dx.doi.org/10.1038/nm0295-118>
- [3] G. Herbein, U. Mählknecht, F. Batliwalla, P. Gregersen, T. Pappas, J. Butler, W. A. O’Brien, and E. Verdin, “Apoptosis of  $CD8^+$  T cells is mediated by macrophages through interaction of HIV gp120 with chemokine receptor CXCR4,” *Nature*, vol. 395, no. 6698, pp. 189–194, 1998. [Online]. Available: <http://dx.doi.org/10.1038/26026>

<sup>8</sup>Interleukins are a group of cytokines (secreted signalling molecules) that are used for ensuring communication between cells. The functions of the immune system strongly depend on interleukins as they provide means of communication (and thus of collaboration) between the different groups of immune system cells.

<sup>9</sup>Indeed, a too important decrease in the value of  $a_{T_1}$  in Figure 4 would bring the system in a parameter region where both eq. point 1 and eq. point 2 coexist. Furthermore, the basin of attraction of eq. point 2 being much larger than the one of eq. point 1, small perturbations on the dynamics typically lead to a situation where the trajectory eventually converges to eq. point 2 (the “non-healthy” eq. point).

- [4] M.-L. Gougeon and L. Montagnier, "Programmed cell death as a mechanism of CD4 and CD8 T cell depletion in AIDS: Molecular control and effect of Highly Active Anti-Retroviral Therapy," *Annals of the New York Academy of Sciences*, vol. 887, no. 1, pp. 199–212, 1999. [Online]. Available: <http://www.blackwell-synergy.com/doi/abs/10.1111/j.1749-6632.1999.tb07934.x>
- [5] A. D. Badley, *Cell Death During HIV Infection*, A. D. Badley, Ed. CRC Press, December 2005. [Online]. Available: <http://www.vonl.com/chips/cellhiv.htm>
- [6] F. Y. Yue, C. M. Kovacs, R. C. Dimayuga, X. X. J. Gu, P. Parks, R. Kaul, and M. A. Ostrowski, "Preferential apoptosis of HIV-1-specific CD4+ T cells," *The Journal of Immunology*, vol. 174, no. 4, pp. 2196–2204, February 2005. [Online]. Available: <http://www.jimmunol.org/cgi/content/abstract/174/4/2196>
- [7] L. Vassena, M. Proschan, A. S. Fauci, and P. Lusso, "Interleukin 7 reduces the levels of spontaneous apoptosis in CD4+ and CD8+ T cells from HIV-1-infected individuals," *Proceedings of the National Academy of Sciences of the United States of America*, vol. 104, no. 7, pp. 2355–60, February 2007.
- [8] A. S. Perelson, P. Essunger, Y. Cao, M. Vesanen, A. Hurley, K. Saksela, M. Markowitz, and D. D. Ho, "Decay characteristics of HIV-1-infected compartments during combination therapy," *Nature*, vol. 387, pp. 188–191, May 1997. [Online]. Available: <http://dx.doi.org/10.1038/387188a0>
- [9] A. S. Perelson and P. W. Nelson, "Mathematical analysis of HIV-1 dynamics in vivo," *SIAM Review*, vol. 41, pp. 3–44, 1999. [Online]. Available: <http://citeseer.ist.psu.edu/perelson98mathematical.html>
- [10] S. Bajaria, G. Webb, and D. Kirschner, "Predicting differential responses to structured treatment interruptions during HAART," *Bulletin of Mathematical Biology*, vol. 66, no. 5, pp. 1093–1118, 2004.
- [11] J. Chen, J.-T. Zhang, and H. Wu, *Computational Science and Its Applications - ICCSA 2005*, ser. Lecture Notes in Computer Science. Springer Verlag Berlin / Heidelberg, 2005, vol. 3483, ch. Discretization Approach and Nonparametric Modeling for Long-Term HIV Dynamic Model, pp. 519–527. [Online]. Available: [http://dx.doi.org/10.1007/11424925\\_55](http://dx.doi.org/10.1007/11424925_55)
- [12] S. Ge, Z. Tian, and T. H. Lee, "Nonlinear control of a dynamic model of HIV-1," *IEEE Transactions on Biomedical Engineering*, vol. 52, no. 3, pp. 353–361, 2005.
- [13] A. Lawen, "Apoptosis-an introduction," *BioEssays : news and reviews in molecular, cellular and developmental biology*, vol. 25, pp. 888–96, Sep. 2003, PMID: 12938178.
- [14] B. Ahr, V. Robert-Hebmann, C. Devaux, and M. Biard-Piechaczyk, "Apoptosis of uninfected cells induced by HIV envelope glycoproteins," *Retrovirology*, vol. 1, p. 12, 2004, PMID: 15214962.
- [15] J. Wang, E. Guan, G. Roderiquez, and M. A. Norcross, "Synergistic induction of apoptosis in primary CD4+ T cells by macrophage-tropic HIV-1 and TGF-beta1," *The Journal of Immunology*, vol. 167, pp. 3360–3366, Sep. 2001. [Online]. Available: <http://www.jimmunol.org/cgi/content/abstract/167/6/3360>
- [16] G. Zauli, D. Gibellini, P. Secchiero, H. Dutartre, D. Olive, S. Capitani, and Y. Collette, "Human immunodeficiency virus Type 1 Nef protein sensitizes CD4+ T lymphoid cells to apoptosis via functional upregulation of the CD95/CD95 ligand pathway," *Blood*, vol. 93, pp. 1000–1010, Feb. 1999. [Online]. Available: <http://bloodjournal.hematologylibrary.org/cgi/content/abstract/bloodjournal;93/3/1000>
- [17] S. A. Stewart, B. Poon, J. Y. Song, and I. S. Y. Chen, "Human immunodeficiency virus Type 1 Vpr induces apoptosis through caspase activation," *The Journal of Virology*, vol. 74, pp. 3105–3111, Apr. 2000. [Online]. Available: <http://jvi.asm.org/cgi/content/abstract/74/7/3105>
- [18] A. Dhooge, W. Govaerts, and Y. Kuznetsov, "Matcont: A MATLAB package for numerical bifurcation analysis of ODEs," *ACM Transactions on Mathematical Software*, vol. 29, pp. 141–164, 2003.
- [19] A. Khibnik, Y. Kuznetsov, V. Levitin, and E. Nikolaev, "Continuation techniques and interactive software for bifurcation analysis of ODEs and iterated maps," *Physica D*, vol. 62, pp. 360–371, 1993.
- [20] E. Doedel, W. Govaerts, Y. Kuznetsov, and A. Dhooge, "Numerical continuation of branch points of equilibria and periodic orbits," *International Journal Bifurcation & Chaos*, vol. 15, pp. 841–860, 2005.
- [21] S. Beq, J.-F. Delfraissy, and J. Theze, "Interleukin-7 (IL-7): immune function, involvement in the pathogenesis of HIV infection and therapeutic potential," *Eur. Cytokine Netw.*, vol. 15, no. 4, pp. 279–289, December 2004.
- [22] C. Fluor, A. D. Milito, T. J. Fry, N. Vivar, L. Eidsmo, A. Atlas, C. Federici, P. Matarrese, M. Logozzi, E. Rajnavolgyi, C. L. Mackall, S. Fais, F. Chiodi, and B. Rethi, "Potential role for IL-7 in Fas-mediated T cell apoptosis during HIV infection," *The Journal of Immunology*, vol. 178, pp. 5340–5350, Apr. 2007. [Online]. Available: <http://www.jimmunol.org/cgi/content/abstract/178/8/5340>